

1 **TITLE:**
2 **Dielectric RheoSANS – Simultaneous Interrogation of Impedance, Rheology and Small**
3 **Angle Neutron Scattering of Complex Fluids**

4
5 **AUTHORS:**

6 Jeffrey J. Richards
7 NIST Center for Neutron Research
8 National Institute of Standards and Technology
9 Gaithersburg, MD, USA
10 Jeffrey.Richards@nist.gov

11
12 Cedric V. L. Gagnon
13 Department of Materials Science and Engineering
14 University of Maryland
15 College Park, MD, USA
16 Cedric.Gagnon@nist.gov

17
18 Jeffery R. Krzywon
19 NIST Center for Neutron Research
20 National Institute of Standards and Technology
21 Gaithersburg, MD, USA
22 Jeffery.Krzywon@nist.gov

23
24 Norman J. Wagner
25 Center for Neutron Science
26 Department of Chemical and Biomolecular Engineering
27 University of Delaware
28 Newark, DE, USA
29 Wagnernj@udel.edu

30
31 Paul D. Butler
32 NIST Center for Neutron Research
33 National Institute of Standards and Technology
34 Gaithersburg, MD, USA
35 Paul.Butler@nist.gov

36
37 **CORRESPONDING AUTHOR:**

38 Norman J. Wagner (wagnernj@udel.edu)

39
40 **KEYWORDS:**

41 Dielectric Spectroscopy, Rheology, Small Angle Neutron Scattering, Electrochemical Flow
42 Cells, Carbon Black, Structure-Property Relationships, Battery.

43
44 **SHORT ABSTRACT:**

45 Here, we present a procedure for the measurement of simultaneous impedance, rheology and
46 neutron scattering from soft matter materials under shear flow.

47

48 **LONG ABSTRACT:**

49 A procedure for the operation of a new Dielectric RheoSANS instrument capable of
50 simultaneous interrogation of the electrical, mechanical and microstructural properties of
51 complex fluids is presented. The instrument consists of a Couette geometry contained within a
52 modified forced convection oven mounted on a commercial rheometer. This instrument is
53 available for use on the small angle neutron scattering (SANS) beamlines at the National
54 Institute of Standards and Technology (NIST) Center for Neutron Research (NCNR). The
55 Couette geometry is machined to be transparent to neutrons and provides for measurement of the
56 electrical properties and microstructural properties of a sample confined between titanium
57 cylinders while the sample undergoes arbitrary deformation. Synchronization of these
58 measurements is enabled through the use of a customizable program that monitors and controls
59 the execution of predetermined experimental protocols. Described here is a protocol to perform a
60 flow sweep experiment where the shear rate is logarithmically stepped from a maximum value to
61 a minimum value holding at each step for a specified period of time while frequency dependent
62 dielectric measurements are made. Representative results are shown from a sample consisting of
63 a gel composed of carbon black aggregates dispersed in propylene carbonate. As the gel
64 undergoes steady shear, the carbon black network is mechanically deformed, which has caused an
65 initial decrease in conductivity associated with the breaking of bonds comprising the carbon
66 black network. However, at higher shear rates, the conductivity recovers associated with the
67 onset of shear thickening. Overall, these results demonstrate the utility of the simultaneous
68 measurement of the rheo-electro-microstructural properties of these suspensions using the
69 Dielectric RheoSANS geometry.

70

71

72 **INTRODUCTION:**

73 Measurement of macroscopic properties are often used to gain fundamental insight into the
74 nature of colloidal materials and self-assembled systems, usually with the goal of developing
75 understanding in order to improve formulation performance. In particular, the field of rheology,
76 which measures a fluid's dynamic response to an applied stress or deformation provides valuable
77 insight into colloidal behavior both under equilibrium conditions, and also far from equilibrium,
78 such as during processing.¹ Rheological tests of consumer and industrial fluids, gels, and glasses
79 can also be used to measure rheological parameters, such as viscosity, that are targeted by
80 formulators. While rheology is a powerful probe of material properties, it is an indirect
81 measurement of colloidal information at the microscopic level, such that our understanding of
82 fundamental colloidal behavior can be greatly enhanced by combining rheological measurements
83 with complementary techniques.

84

85 One such orthogonal technique is impedance spectroscopy. Impedance spectroscopy is a bulk
86 probe of dielectric relaxation behavior, which measures the response of a material to an applied
87 oscillating electric field.² The impedance spectrum results from electrical relaxation modes that
88 are active within the material including charge transport and polarization.^{3,4} These measurements
89 provide additional evidence for colloidal behavior particularly when combined with rheology.⁵
90 Therefore, the combination of these techniques is especially relevant when probing charged
91 colloidal dispersions, proteins, ionic surfactants, nanocomposites, and other systems.^{6,7}

92

93 A fundamental interest in investigations of colloidal behavior is the material's microstructure.
94 The microstructure of a colloidal fluid is thought to encode all of the information necessary to
95 reconstitute both its rheological and electrical behavior. Fundamentally, we seek to measure a
96 snapshot of the nanoscale microstructural features that lead to a measured material response. Due
97 to the complicated nature of many complex fluids' dependence on their process history, much of
98 the effort on microstructural characterization has focused on making in situ measurements of the
99 material as it undergoes deformation. This has challenged experimentalists to devise methods to
100 be able to make measurements of nano-sized particles under for example steady shear, where the
101 velocities of the particles have made direct visualization intrinsically challenging. Direct
102 measurement of material microstructure under flow has taken on many forms ranging from rheo-
103 optics, rheo-microscopy and even rheo-NMR.⁸⁻¹⁰ Small angle scattering methods, and in
104 particular small angle neutron scattering (SANS) techniques, have proven themselves effective at
105 measuring the time-averaged microstructure of samples at steady state in a bulk shear field
106 including all three planes of shear.¹¹⁻¹³ However, new data acquisition techniques have allowed
107 structural transients to be captured with time resolution as fine as 10 ms.¹⁴ Indeed combining
108 rheology with various in situ scattering methods has proven invaluable in hundreds of recent
109 studies.¹⁵

110
111 An emerging engineering challenge is the use of colloidal suspensions as conductive additives in
112 semi-solid flow battery electrodes.¹⁶ In this application, conductive colloidal particles must
113 maintain an electrically percolated network while the material is pumped through an
114 electrochemical flow cell. The performance demands on these materials require that they
115 maintain high conductivity without detrimental effect on the rheological performance over a
116 wide range of shear rates.¹⁷ It is therefore highly desirable to be able to make measurements of
117 the colloidal behavior under steady and time-dependent shear conditions in order to quantify and
118 characterize the underlying rheological and electrical response of these materials far from their
119 equilibrium state. A significant complicating factor that has hindered further theoretical
120 development in this regard is the thixotropic nature of carbon black slurries.¹⁸ These history
121 dependent rheological and electrical properties make experiments notoriously difficult to
122 reproduce; thus, making it difficult to compare data sets measured using varying protocols.
123 Furthermore, to date there is no single geometry capable of performing all three, dielectric,
124 rheological, and microstructural characterizations, simultaneously. Simultaneous measurement is
125 important as the flow can change the structure, such that rest measurements of processed
126 materials may not provide accurate indications of the properties under flow, which are more
127 relevant for their use. Additionally, as many of the measured properties of carbon black slurries
128 are geometry dependent, there are complications with comparing data obtained from the same
129 sample on different instruments.¹⁹

130
131 In order to meet this challenge in metrology, we have developed a new Dielectric RheoSANS
132 geometry at the NIST Center for Neutron Research and the University of Delaware capable of in
133 situ impedance spectroscopy, rheology and SANS measurements of a material under arbitrary
134 deformation on a commercial strain controlled rheometer. This is enabled by developing a
135 Couette geometry capable of measuring the microstructural, electrical and rheological response
136 of a material confined between the gap of two concentric cylinders. As the outer cylinder spins,
137 torque imposed by the deformation of the sample is measured on the inner cylinder and the
138 impedance measurement is made radially across the gap. The cylinders are machined from

139 titanium so as to be transparent to neutrons and robust enough to withstand the shear stress
140 experienced in the rheometer. We perform the SANS measurement through the radial position of
141 the Couette, and have demonstrated that it is possible to measure high quality SANS patterns
142 from the sample undergoing deformation. In this way, all three measurements are made on the
143 same region of interest in the sample as it undergoes a well-defined deformation profile. The
144 goal of this article is to describe the Dielectric Couette Geometry, its installation onto the
145 RheoSANS instrument, and the successful execution of a simultaneous measurement. This
146 rheometer is available at the NIST Center for Neutron Research at the National Institute of
147 Standards and Technology. It has been designed to work on the NG-7 SANS beam line. We have
148 provided drawings and a detailed description of the custom components that have been machined
149 and assembled in order to enable this measurement.

150

151 **PROTOCOL:**

152

153 **1. Mounting the Rheometer onto the SANS Beamline.**

154 Note: See Figure 1 for definitions of named components.

155

156 1.1) Ensure that the power to the rheometer is off, the transducer is locked and the motor air
157 bearing protector is installed, turn off the neutron beam, and close the oven door.

158

159 1.2) Install large base plate onto Table, remove the snout, install the window, and secure the 4
160 eyelets to the mounting brackets on the rheometer's crane adapter such that the cables do not
161 tangle and are not twisted.

162

163 1.3) Using the crane, lift Rheometer and maneuver it from the Rheometer table to rest
164 centered on the Table with the LCD screen of the Rheometer facing outward taking care to guide
165 the cables to minimize tangling.

166

167 1.4) Using the SANS control software, send Ttable to minimum Z position.

168

169 1.5) Remove the rheometers' crane adapter and lift away from the platform using the crane.

170

171 **2. Dielectric Cell Assembly**

172 Note: See Figure 2 for definitions of named components.

173

174 2.1) Ensure that the power to the rheometer is off, the transducer is locked and the motor air
175 bearing protector is installed. Clean Dielectric Cup and Bob Assemblies before use using
176 detergent solution followed by several deionized water rinses, and allow to fully dry.

177

178 2.2) Open the oven door, unlock the transducer and remove the motor bearing lock, and
179 mount the Dielectric Geometry and Dielectric Bob Assembly onto the upper and lower tool
180 mounts of the Rheometer. Loosen both set screws on the Dielectric Geometry using a 2 mm
181 Allen key and place the Dielectric Cup Assembly so that it is mounted on the Dielectric
182 Geometry.

183

184 2.3) Using the rheometer control software, zero the gap from the sample geometry drop-down
185 menu, and apply 10 N Normal Force using the Axial Force drop-down menu. Under
186 compression, tighten screws using a 3 mm Allen key until Dielectric Cup Assembly is fully
187 secured to Dielectric Geometry.

188
189 2.4) Set the gap to the measurement gap using rheometer control software, and close the oven
190 door. Ensure that the oven can fully enclose the Dielectric Cell with adequate vertical clearance
191 on the top and bottom of the geometry. If height adjustment is needed, adjust the set screw so
192 that the oven enclosure fits with adequate tolerance around the Dielectric Cell. Adequate
193 clearance is achieved when the Dielectric Geometry fits within the oven and can undergo a full
194 revolution without touching the oven walls.

195
196 2.5) Remove both the Dielectric Bob Assembly and the Dielectric Cup Assembly/Dielectric
197 Geometry as one piece and replace with the Rheometer Alignment tool on the lower tool head.

198 3. **Install the Slip Ring**

199 Note: See Figure 3 for Step by Step Pictorial Summary.

200
201
202 3.1) Install the Wire Baffle onto the shaft of the Dielectric Geometry and connect the
203 Dielectric Cup Connector to the Slip Ring Connector.

204
205 3.2) Hold the Slip Ring so that it is concentric with the shaft of the Dielectric Cup
206 Assembly/Dielectric Geometry but above the flange on the Dielectric Geometry. Place the Slip
207 Ring Adapters (x2) such that their nobs insert into the holes drilled into the Dielectric Geometry
208 and their base rests on the Dielectric Geometry flange.

209
210 3.3) Gently slide the Slip Ring Over the Slip Ring Adapters. The Slip Ring should slide
211 effortlessly around the Slip Ring Adapters holding them in place.

212 4. **Alignment of the Rheometer.**

213 Note: See Figure 4 for Schematic of Beam Path.

214
215
216 4.1) Close the oven around the Rheometer Alignment tool. Install the truncated snout and the
217 sample aperture (1mm wide \times 8 mm tall), and using rheometer control software, set the geometry
218 displacement angle to 0.49 rad in the motor control drop-down menu.

219
220 4.2) Using the SANS instrument control software, ensure that all the neutron guides are
221 removed, and open the oven door so that the laser is visible. Perform a rough alignment of the
222 rheometer by changing the height and angle of the table from the SANS instrument control
223 software so that the beam passes through the oven and crosses through the slit in the center of the
224 Rheometer Alignment Tool.

225
226 4.3) Using the SANS instrument control software, adjust the height of the table and its
227 rotation to optimize laser alignment. Note the rheometer is aligned when the laser beam passes
228 through the slit in the Rheometer Alignment Tool with the geometry displacement set at 0.49 rad
229 without impinging on its walls and the beam passes through the center line in the oven.

230
231
232
233
234
235
236
237
238
239
240
241
242
243
244
245
246
247
248
249
250
251
252
253
254
255
256
257
258
259
260
261
262
263
264
265
266
267
268
269
270
271
272
273

5. Calibration of the SANS instrument

5.1) Once the desired SANS instrument configuration is aligned by the instrument scientist, measure the Open Beam Transmission, Empty Cell Scattering, and Dark Current Scattering measurements. The Open Beam transmission measurement is performed by performing a beam transmission measurement at the desired detector position for three minutes. The Empty Cell Scattering measurement is performed by installing the Dielectric Geometry and measuring a scattering measurement at the desired detector position. Finally, the Dark Current Scattering measurement is performed using a 3 mm thick piece of cadmium that totally attenuates the main beam scattering signal.

5.2) Uninstall the Dielectric Geometry, and measure the Open Beam transmission through the oven with the oven door closed at the desired configuration. Measure the Dark Current Scattering by hanging a 3 mm thick cadmium slab in the beam path and performing a scattering measurement using the same configuration.

5.3) Finally, reinstall the Dielectric Geometry, and perform a scattering measurement through the oven with the door closed.

6. Connecting the Electric Components

6.1) Set the gap using the LCD screen to 100 mm.

6.2) Remove the Rheometer Alignment Tool from the bottom tool flange. Reinstall the Dielectric Bob Assembly on the upper tool head and the Dielectric Cup Assembly/Dielectric Geometry/Slip Ring Assembly onto the lower tool head as one piece and re-zero the gap.

6.3) Ensure that the Carbon Brush Assembly is secured to the Carbon Brush Adapter using screws, and secure the Carbon Brush Adapter and Carbon Brush Assembly to the rheometer using screws. Ensure that the carbon brushes on the Carbon Brush Assembly mate with the grooved metal rings of the Slip Ring. This ensures maintenance of electrical contact.

6.4) Connect the female pin connectors on the Carbon Brush Assembly and the Dielectric Bob Assembly to the male pin connectors of the top and bottom bus bars respectively. Ensure that the labeled shielded BNC cables connected to the bus bars and terminating at the LCR meter are installed in their corresponding BNC connectors.

6.5) Connect the BNC cable labeled "TO SANS" to the BNC cable connected to the DAQ card labeled "AO0". Connect the BNC cable labeled "FROM SANS" to the BNC cable connected to the DAQ card labeled "AI0". Connect the BNC cable labeled "TRIGGER" to the BNC cable connected to the DAQ card labeled "AO1". Connect the BNC cable connected to the 15 pin connector on the back of the Rheometer to the BNC cable labeled "AI3". Ensure the LCR meter and Rheometer are communicating with the control computer.

7. Preparing the Instrument for a Measurement

274 7.1) Open Oven, set the Gap to 100 mm, and load 4 mL of carbon black dispersion in
275 propylene carbonate into the temperature equilibrated Dielectric Cup Assembly taking care to
276 minimize sample left on the Cup Wall.

277
278 7.2) Lower the Geometry to 40 mm using the Front LCD Screen. Set the velocity on the
279 rheometer control software using the motor control settings to 1 rad/s. Using the slew option on
280 the rheometer, lower the Dielectric Bob Assembly until the gap distance is at 0.5 mm.

281
282 7.3) Using the equipment software, go to Dielectric Geometry measurement gap, and set the
283 motor velocity on rheometer control software using the motor control settings to 0 rad/s. At this
284 stage, the sample is loaded. **Note:** check the sample fill level once more to ensure that the sample
285 level fills all the way up the Couette wall without overflowing.

286
287 7.4) Install the Solvent Trap by filling the inner Dielectric Bob Assembly Wall with the
288 desired solvent and place the solvent trap on the rim of the Dielectric Cup Assembly.

289

290 8. Running the Dielectric RheoSANS Experiment

291 8.1) Configure code Labeled “TA_ARES_FlowSweep.vi”. A GUI will appear with
292 modifiable fields that specify the experimental run conditions of the Dielectric RheoSANS
293 experiment. Set these fields in the following order.

294

295 8.1.1) Specify a path for the log file to and the base name of the log file. Run the code by
296 pressing the “Run” arrow button on the menu bar.

297

298 8.1.2) Select Rheological Parameters – the starting shear rate (25 rad/s), ending shear rate (1
299 rad/s), the number of shear rate points (6) and whether the points should be logarithmically or
300 linear spaced (radio button). Select Temperature - 25°C for this experiment. Select Preshear
301 Conditions (if desired, enable radio button to “ON”) – in this experiment we use a 25 rad/s
302 preshear for 600 seconds with a 300 second wait time after the preshear step

303

304 8.1.3) Specify Time per Shear Rate and Collection Rate. Enable Handshaking radio button. On
305 Test Parameters Tab Select Logarithmic or Linear Sweep – if radio button is green, a list of N
306 number of points will be logarithmically spaced from min shear rate to max shear rate.

307

308 8.1.4) Specify Discrete Shear Rates and Times via the “Discrete Values” tab if desired. Select
309 number of frequency points, frequency minimum and frequency maximum default. Set Time
310 Dependent Frequency – specifies the desired time dependent frequency for all shear rates. Set
311 Time for Steady State – sets the amount of time that the code will measure dielectric parameters
312 at a fixed frequency as a function of time for each shear rate.

313

314 8.1.5) Specify the signal type and amplitude. Specify the number of cycles to average and the
315 measurement time.

316

317 8.2) Turn on AutoLogging on the SANS computer. Set SANS Configuration. Select
318 configuration and specify run time to be at least 1 minute longer than the total time contained
319 within the shear rate list in the Code. **Note:** When the configuration is achieved VIPER should

320 read “dio stat 16” which indicates that it will be waiting for the Analogue Signal from the data
321 acquisition card to change.

322

323 8.3) Configuring rheometer control software. In the experiment tab, Press “Open Procedure
324 File” in the “Procedure” drop down menu. Navigate to the Procedure File Labeled “Dielectric
325 RheoSANS Script File”. Ensure that Rheometer is ready to execute experiment.

326

327 8.4) When the SANS is ready, ensure control software is configured and rheometer control
328 software script file is open, Press “Parameters Set”. This triggers execution of the specified
329 experiment and all data should be logged throughout the preprogrammed sample run.

330

331 9. End of Experiment

332 9.1) Turn off the neutron beam and disable Auto-Logging. Unload the sample and remove the
333 Dielectric Cup and Bob Assemblies from the rheometer. Install the motor air bearing protector
334 and lock the transducer.

335

336 9.2) Power down the computer, LCR Meter, and rheometer power supplies. Disconnect the air
337 line. Disconnect all BNC Cables and reinstall the crane lift onto the rheometer.

338

339 9.3) Uninstall the truncated snout. Reinstall the rheometer’s crane adapter. Lift the rheometer
340 from the table and place onto the rheometer table ensuring that the cables remain untangled.

341

342 [Place Figure 1-4 here]

343

344 REPRESENTATIVE RESULTS:

345 Representative results from a Dielectric RheoSANS experiment are shown in Figure 5 and 6.

346 These data are taken on a suspension of conductive carbon black in propylene carbonate. These

347 aggregates flocculate due to attractive interactions at relatively low solids loadings forming gels

348 that are electrically conducting. The rheological and conductivity responses of such suspensions

349 are an active area of research and current investigations seek to understand the microstructural

350 origins of these measurements. The Dielectric RheoSANS instrument is a tool uniquely suited to

351 address this question as it probes simultaneously the electrical and mechanical properties of a

352 material as it undergoes deformations similar to those found in an application such as in a semi-

353 solid electrochemical flow cell. In such a cell the carbon black forms the conducting additive that

354 provides volumetric conductivity to the flowing electrodes.

355

356 The experiment outlined in the procedure is designed to test a conductive material as it

357 undergoes a flow sweep test, where the shear rate is stepped logarithmically from a maximum

358 value to a minimum value holding at each shear rate for a specified period of time. Rheology,

359 dielectric data and neutron scattering are measured continuously during the course of this

360 experimental sequence. Upon completion of a Dielectric RheoSANS experiment, the data is

361 stored in three independent formats. The SANS data is stored as an event mode file that is a

362 binary file generated by the detector containing the list of the time of arrival of each neutron on

363 the detector and the x, y position of the pixel on which it was detected. The rheology data is

364 stored within the rheometer control software as a separate data file and can be exported as a

365 column delimited text file containing the relevant rheological parameters (i.e. torque, shear rate,

366 and normal force). Finally, the dielectric data is contained within the log file written by the
367 control interface to the specified folder that records the impedance magnitude and phase shift as
368 a function of the applied frequency. The first post-processing task is to synchronize and then sort
369 the raw data. A detailed description of this process is published elsewhere, but briefly, the
370 synchronization is made possible by a data acquisition card that monitors a digital signal from
371 the rheometer and uses an analogue triggering protocol to encode measurement condition
372 transitions into the SANS detector clock time.²⁰ Using this approach, the raw measured signals
373 from the SANS, rheometer and LCR meter can be reconstructed as a function of both shear rate
374 and time.

375
376 After the raw signals are sorted, they are corrected using the known rheological and electrical
377 cell constants and using standard SANS reduction methods. The dielectric data correction and
378 analysis procedure is shown in Figure 5a after removing the open and short circuit measurements
379 at each frequency and shear rate. Once corrected the dielectric signals are converted to the real
380 and imaginary components of the impedance versus frequency. In figure 5a, there is a plot of
381 Nyquist representation of dielectric measurement of an 0.08 weight fraction Vulcan XC72R
382 sample undergoing steady shear averaged over the last 900s of the acquisition. In the Nyquist
383 representation the real and complex components of the impedance are plotted parametrically
384 against one another. On the top left plot, the data points are logarithmically colorized by the
385 frequency at which the measurement is taken with yellow representing the highest frequency (20
386 MHz) and black representing the lowest accessible frequency (20 Hz). In the middle plot, the
387 sample admittance, Y^* , or the inverse of the complex impedance, Z^* , is plotted against the
388 frequency. It is normalized by the known cell constant, λ , and the sample conductivity and
389 electrical susceptibility are defined as the imaginary and real components of the admittance. This
390 normalized sample response can be converted to the complex permittivity, ϵ^* , by dividing the
391 admittance by $2\pi f\epsilon_0$. Finally, we fit the complex permittivity of the sample response using the
392 dielectric response model as a sum of a Havriliak-Nagami Relaxation and a Constant Phase
393 Element that accounts for the effects of electrode polarization.²⁰

394
395 [Place Figure 5 here]

396
397 The raw event mode data is histogrammed with respect to time onto the two-dimensional SANS
398 detector representing $I(Q_x, Q_y)$. This raw signal intensity is then corrected for the empty cell,
399 blocked beam, and transmission and converted to absolute scale with units cm^{-1} . After these
400 corrections, the absolute intensity can be plotted as a function of shear rate and time. In Figure
401 5b, on the left, the two-dimensional reduced scattering intensity versus Q_x and Q_y is plotted. In
402 the middle we plot the form factor, $P(Q)$, scaled by a prefactor, A , of the model fit to the dilute
403 carbon black suspension over an identical Q -range. We then divide $I(Q)$ by $A \cdot P(Q)$ to obtain
404 $S(Q)$ which represents an apparent structure factor for the interactions between the fractal carbon
405 black aggregates that comprise the sample. Next the two-dimensional $S(Q)$ plot is integrated at
406 the minimum accessible Q value $= 0.0015 \text{ \AA}^{-1}$ to calculate S_0 , which is an estimate of the apparent
407 repulsive interaction between fractal aggregates. This result is then converted to an equivalent
408 hard sphere volume fraction.

409
410 Using this approach, the steady-state data can be analyzed at each shear rate and the extracted
411 parameters that result from both the structural analysis and the dielectric analysis can be plotted

412 as a function of the applied shear rate and rheological shear stress as shown in Figure 6. Also
413 plotted are the two-dimension $S(Q)$ plots for several shear rates of interest that mark important
414 microstructural transitions. Because these values are all measured at the same time from the
415 same region within the Couette, they can be directly compared and correlated. This is
416 emphasized by the fact that transitions in conductivity, κ_{LF} , and effective volume fraction, ϕ_{HS} ,
417 correspond with the increase of stress when the shear stress exceeds the yield stress marked by
418 the transition from region I-II. In this transition, both ϕ_{HS} and κ_{LF} decrease which is associated
419 with the yielding of the macroscopic gel. As the shear rate is further increased, the sample shear
420 thickens as indicated by the apparent increase in the viscosity and the κ_{LF} increases while ϕ_{HS}
421 continues to decrease. This transition is marked by region II-III. For concentrated colloidal
422 suspensions, shear thickening is associated with the formation of large structures that form as
423 result of hydrodynamic interactions imposed by the flow of the bulk fluid around the primary
424 carbon black particles. These hydrodynamic forces draw the aggregates together resulting in an
425 abrupt increase in conductivity and viscosity.

426

427 [Place Figure 6 here]

428

429 The technical schematics of the key components of the Dielectric RheoSANS geometry shown in
430 Figure 2 are provided in Supplementary Figures 1-8, such that this geometry can be reproduced
431 on similar strain controlled rheometers.

432

433 **Figure 1:** a.)-e.) Pictures of Components of the SANS beamline and the Rheometer necessary to
434 Install rheometer on the beamline that are labelled and defined below.

435

436 **Figure 2:** a.)-e.) Pictures of components Dielectric RheoSANS geometry with labels defining
437 terms below.

438

439 **Figure 3:** a.-d.) Pictures of Procedure for Installing the Slip-Ring onto the Dielectric RheoSANS
440 Geometry, and e.) Picture of fully assembled Dielectric RheoSANS Geometry.

441

442 **Figure 4:** Schematic of Beam Path through Oven Geometry and Dielectric RheoSANS
443 Geometry.

444

445 **Figure 5:** a.) Summary of Dielectric Data Analysis; *left* Nyquist Representation, *middle:*
446 Conductivity and Susceptibility vs frequency, *right:* Complex Permittivity versus Frequency –
447 Dielectric Model accounts for electrode polarization and Havriliak-Negami Relaxation shown
448 overlaid on top of data, b.) Summary of SANS Data Analysis; *left:* $I(Q)$ from 0.08 weight
449 fraction Vulcan XC72R at 1 rad/s averaged for last 900s of shear rate, *middle:* scaled model fit to
450 dilute sample $P(Q)$, *right:* sample structure factor, $S(Q)=I(Q)/(A \cdot P(Q))$ – red circle denotes Q -
451 position position where data is averaged to obtain the minimum structure factor depth, S_0 .

452

453 **Figure 6:** *top:* two-dimensional $S(Q)$ plots at shear rates that represent important microstructural
454 transitions in the sample, *bottom:* summary of rheological (shear stress), dielectric (static
455 permittivity and low frequency conductivity) and SANS parameters (scale factor and effective
456 excluded volume fraction) as a function of applied shear rate. The regions of interests are marked
457 as I-III. In region I, creep maintains an interconnected network structure. In region II, the gel

458 macroscopically yields leading to a decrease in the overall conductivity. In region III, there is an
459 apparent shear thickening resulting in clustering and an increase in conductivity. Error bars
460 represent one standard deviation of the average.

461
462 [Place Supplementary Figure 1 here]

463
464 **Supplementary Figure 1:** Technical Schematic of the Dielectric Cup Adapter.

465
466 [Place Supplementary Figure 2 here]

467
468 **Supplementary Figure 2:** Technical Schematic of the Dielectric Cup Wall.

469
470 [Place Supplementary Figure 3 here]

471
472 **Supplementary Figure 3:** Technical Schematic of the Dielectric Bob Wall.

473
474 [Place Supplementary Figure 4 here]

475
476 **Supplementary Figure 4:** Technical Schematic of the Dielectric Bob Shaft.

477
478 [Place Supplementary Figure 5 here]

479
480 **Supplementary Figure 5:** Technical Schematic of the Dielectric Bob Cap.

481
482 [Place Supplementary Figure 6 here]

483
484 **Supplementary Figure 6:** Technical Schematic of the Dielectric Bob Assembly.

485
486 [Place Supplementary Figure 7 here]

487
488 **Supplementary Figure 7:** Technical Schematic of the Slip Ring Adapter.

489
490 [Place Supplementary Figure 8 here]

491
492 **Supplementary Figure 8:** Technical Schematic of the Carbon Brush Adapter.

493
494 **DISCUSSION:**

495 A Dielectric RheoSANS experiment measures simultaneously the rheological, electrical and
496 microstructural responses of a material as it undergoes a predefined deformation. The example
497 shown here is an electrically conductive carbon black suspension that forms the conductive
498 additive used in electrochemical flow cells. The Dielectric RheoSANS instrument enables the
499 interrogation of the radial plane of shear within a narrow gap Couette cell without compromising
500 the fidelity of either the electrical or rheological measurement. Additionally, the geometry allows
501 for conversion of raw signals, torque, resistance, and phase shift, to appropriate intrinsic
502 variables such as shear stress, conductivity and permittivity. In the experiment outlined in this
503 procedure, a flow sweep is performed where the shear rate is logarithmically stepped from a

504 maximum value to a minimum value while the time-dependent and shear rate dependent rheo-
505 electro-structural properties are recorded. From this measurement, it is possible to examine the
506 evolution of microstructure and conductivity of the carbon black gel as it yields and then
507 undergoes macroscopic flow. Because of the simultaneous dielectric measurement, we are able
508 to probe the origin of conduction in these gelled materials far from equilibrium as they melt.²⁰ A
509 flow sweep is just one type of potential test that can be performed, and the geometry is design to
510 accommodate a wide range of potential time-dependent shear profiles. These results have a
511 potential to improve the performance of flow battery electrodes by guiding the formulation of
512 low-viscosity, high conductivity fluids.²¹

513
514 A critical enabling component of a Dielectric RheoSANS experiment is the synchronization of
515 all three measurements. Synchronization allows all three measurement characteristics to be
516 compared as a function of time and shear rate. This is made possible by the analogue triggering
517 protocol that encodes transitions in shear rate in the neutron arrival time. This protocol exploits
518 event mode acquisition of the SANS detector which generates a continuous list of the arrival
519 time and pixel position of each neutron detected. The detector clock time can be reset using an
520 analogue trigger, a 10 ms pulse with a 5 V amplitude. This resets the absolute arrival time of the
521 neutrons within that list. The protocol outlined above allows this clock to be reset at the moment
522 the motor is turned on and between each shear rate. This synchronization protocol allows the
523 user to reconstitute the microstructural evolution of the sample to a time-resolution of 100 ms.
524 An important limitation of this method is that currently there is no way to change detector
525 position during the course of an acquisition. Therefore, only a single detector position can be
526 acquired for a given experimental protocol. This will be improved by upcoming software
527 changes in both the rheometer control protocols as well as the SANS instrument operations.

528
529 The results provided by this new instrument open up a new path to interrogate electrically active
530 colloidal materials as they undergo deformation. In contrast to existing rheo-electric, rheo-
531 SANS, and dielectric-SANS geometries, the Dielectric RheoSANS geometry described here is
532 capable of simultaneous dielectric-SANS measurement under arbitrary applied shear fields. This
533 technique has relevance not only to electrochemical flow cells but the development of fuel cell
534 electrodes and other electronic devices where materials are processed from the solutions state
535 and subject to macroscopic shear.²²⁻²⁴ The instrument also has relevance to the study of materials
536 whose mechanical properties can be actuated via an applied electric field. All these applications
537 can potentially be studied by virtue of the flexible design of this instrument and the methodology
538 for synchronizing the execution of each testing protocol.

539
540 Work is ongoing to improve the protocols for executing a Dielectric RheoSANS experiment and
541 creating new testing methodologies for a wider range of materials. Additionally, improved
542 atmospheric control will be enabled with the improvement of the oven design and upcoming
543 replacement of the window material within the oven environment. This will include an improved
544 solvent trap design that will make long duration experiments on volatile fluids feasible.
545 Upcoming oven designs promise access to the tangential plane of shear which has been
546 demonstrated in operating RheoSANS instruments, but is not currently a tested and proven
547 capability of the Dielectric RheoSANS instrument.

548
549 **ACKNOWLEDGMENTS:**

550 The authors would like to acknowledge the NIST Center for Neutron Research CNS cooperative
551 agreement number #70NANB12H239 grant for partial funding during this time period as well as
552 the National Research Council for support. Certain commercial equipment, instruments, or
553 materials are identified in this paper in order to specify the experimental procedure adequately.
554 Such identification is not intended to imply recommendation or endorsement by the National
555 Institute of Standards and Technology, nor is it intended to imply that the materials or equipment
556 identified are necessarily the best available for the purpose.

557

558 **DISCLOSURES:**

559 The authors have nothing to disclose.

560

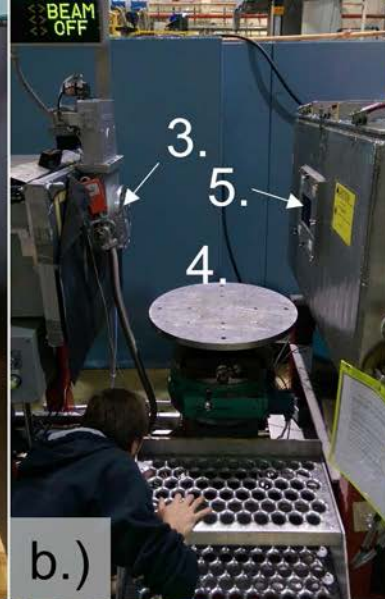
561 **REFERENCES**

- 562 1. Macosko, C. *Rheology: Principles, Measurements and Applications*. Powder Technology
563 **86** (3), doi:10.1016/S0032-5910(96)90008-X (1996).
- 564 2. Barsoukov, E. & Macdonald, J. R. *Impedance Spectroscopy Theory, Experiment, and*
565 *Applications*. Wiley-Interscience (2010).
- 566 3. Pelster, R. & Simon, U. Nanodispersions of conducting particles: Preparation,
567 microstructure and dielectric properties. *Colloid Polym. Sci.* **277** (1), 2–14,
568 doi:10.1007/s003960050361 (1999).
- 569 4. Hollingsworth, A. D. & Saville, D. A. Dielectric spectroscopy and electrophoretic
570 mobility measurements interpreted with the standard electrokinetic model *J. Colloid*
571 *Interface Sci.* **272** (1), 235–245, doi:10.1016/j.jcis.2003.08.032 (2004).
- 572 5. Mewis, J. & Spaul, A. J. B. Rheology of concentrated dispersions. *Adv. Colloid Interface*
573 *Sci.* **6** (3), 173–200, doi:10.1016/0001-8686(76)80008-5 (1976).
- 574 6. Mijović, J., Lee, H., Kenny, J. & Mays, J. Dynamics in Polymer–Silicate Nanocomposites
575 As Studied by Dielectric Relaxation Spectroscopy and Dynamic Mechanical Spectroscopy.
576 *Macromolecules* **39** (6), 2172–2182, doi:10.1021/ma051995e (2006).
- 577 7. Newbloom, G. M., Weigandt, K. M. & Pozzo, D. C. Electrical, Mechanical, and
578 Structural Characterization of Self-Assembly in Poly(3-hexylthiophene) Organogel
579 Networks. *Macromolecules* **45** (8), 3452–3462, doi:10.1021/ma202564k (2012).
- 580 8. Fowler, J. N., Kirkwood, J. & Wagner, N. J. Rheology and microstructure of shear
581 thickening fluid suspoemulsions. *Appl. Rheol.* **24** (4), 23049 (2014).
- 582 9. Wagner, N. J. Rheo-optics. *Curr. Opin. Colloid Interface Sci.* **3** (4), 391–400,
583 doi:10.1016/S1359-0294(98)80055-1 (1998).
- 584 10. Callaghan, P. T., *et al.* Rheo-NMR: nuclear magnetic resonance and the rheology of
585 complex fluids. *Reports Prog. Phys.* **62** (4), 599–670, doi:10.1088/0034-4885/62/4/003
586 (1999).
- 587 11. Gurnon, A. K., Godfrin, P. D., Wagner, N. J., Eberle, A. P. R., Butler, P. & Porcar, L.
588 Measuring Material Microstructure Under Flow Using 1-2 Plane Flow-Small Angle
589 Neutron Scattering. *J. Vis. Exp.* (84), e51068–e51068, doi:10.3791/51068 (2014).
- 590 12. Calabrese, M. A., Rogers, S. A., Murphy, R. P. & Wagner, N. J. The rheology and
591 microstructure of branched micelles under shear. *J. Rheol.* **59** (5), 1299–1328,
592 doi:10.1122/1.4929486 (2015).
- 593 13. Helgeson, M. E., Vasquez, P. A., Kaler, E. W. & Wagner, N. J. Rheology and spatially
594 resolved structure of cetyltrimethylammonium bromide wormlike micelles through the
595 shear banding transition. *J. Rheol.* **53** (3), 727, doi:10.1122/1.3089579 (2009).

- 596 14. Calabrese, M. A., *et al.* An optimized protocol for the analysis of time-resolved elastic
597 scattering experiments. *Soft Matter* **12** (8), 2301–2308, doi:10.1039/C5SM03039K
598 (2016).
- 599 15. Eberle, A. P. R. & Porcar, L. Flow-SANS and Rheo-SANS applied to soft matter. *Curr.*
600 *Opin. Colloid Interface Sci.* **17** (1), 33–43, doi:10.1016/j.cocis.2011.12.001 (2012).
- 601 16. Campos, J. W., *et al.* Investigation of carbon materials for use as a flowable electrode in
602 electrochemical flow capacitors. *Electrochim. Acta* **98**, 123–130,
603 doi:10.1016/j.electacta.2013.03.037 (2013).
- 604 17. Duduta, M., *et al.* Semi-solid lithium rechargeable flow battery. *Adv. Energy Mater.* **1** (4),
605 511–516, doi:10.1002/aenm.201100152 (2011).
- 606 18. Mewis, J., de Groot, L. M. & Helsen, J. A. Dielectric Behaviour of Flowing Thixotropic
607 Suspensions. *Colloids Surf.* **22**, 271–289, doi:10.1016/0166-6622(87)80226-3 (1987).
- 608 19. Helal, A., Divoux, T. & McKinley, G. H. Simultaneous rheo-electric measurements of
609 strongly conductive complex fluids. at <<http://arxiv.org/abs/1604.00336>> (2016).
- 610 20. Richards, J. J., Hipp, J., Wagner, N. J. & Butler, P. D. Dielectric RheoSANS: The Study
611 of Electrical and Mechanical Properties of Complex fluids. *Rev. Sci. Instr.* **In prepara**
612 (2016).
- 613 21. Youssry, M., Madec, L., Soudan, P., Cerbelaud, M., Guyomard, D. & Lestriez, B. Non-
614 aqueous carbon black suspensions for lithium-based redox flow batteries: rheology and
615 simultaneous rheo-electrical behavior. *Phys. Chem. Chem. Phys. PCCP* **15** (34), 14476–
616 86, doi:10.1039/c3cp51371h (2013).
- 617 22. Cho, B.-K., Jain, A., Gruner, S. M. & Wiesner, U. Mesophase structure-mechanical and
618 ionic transport correlations in extended amphiphilic dendrons. *Sci. (New York, N.Y.)* **305**
619 (5690), 1598–601, doi:10.1126/science.1100872 (2004).
- 620 23. Kiel, J. W., MacKay, M. E., Kirby, B. J., Maranville, B. B. & Majkrzak, C. F. Phase-
621 sensitive neutron reflectometry measurements applied in the study of photovoltaic films. *J.*
622 *Chem. Phys.* **133** (7), 1–7, doi:10.1063/1.3471583 (2010).
- 623 24. López-Barrón, C. R., Chen, R., Wagner, N. J. & Beltramo, P. J. Self-Assembly of
624 Pluronic F127 Diacrylate in Ethylammonium Nitrate: Structure, Rheology, and Ionic
625 Conductivity before and after Photo-Cross-Linking. *Macromolecules* **49** (14), 5179–5189,
626 doi:10.1021/acs.macromol.6b00205 (2016).



a.)



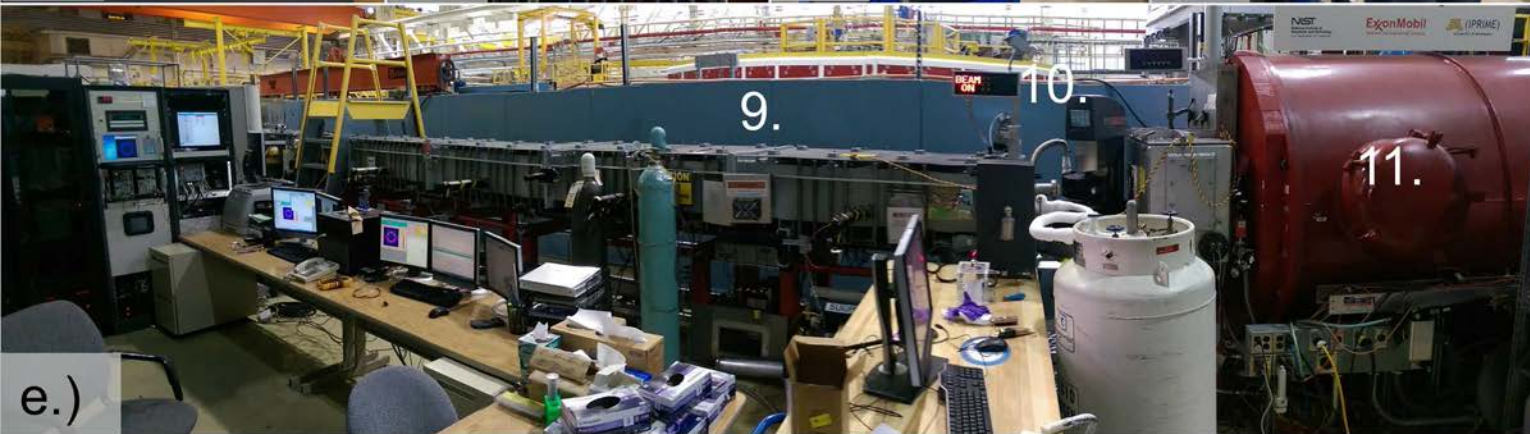
b.)



c.)

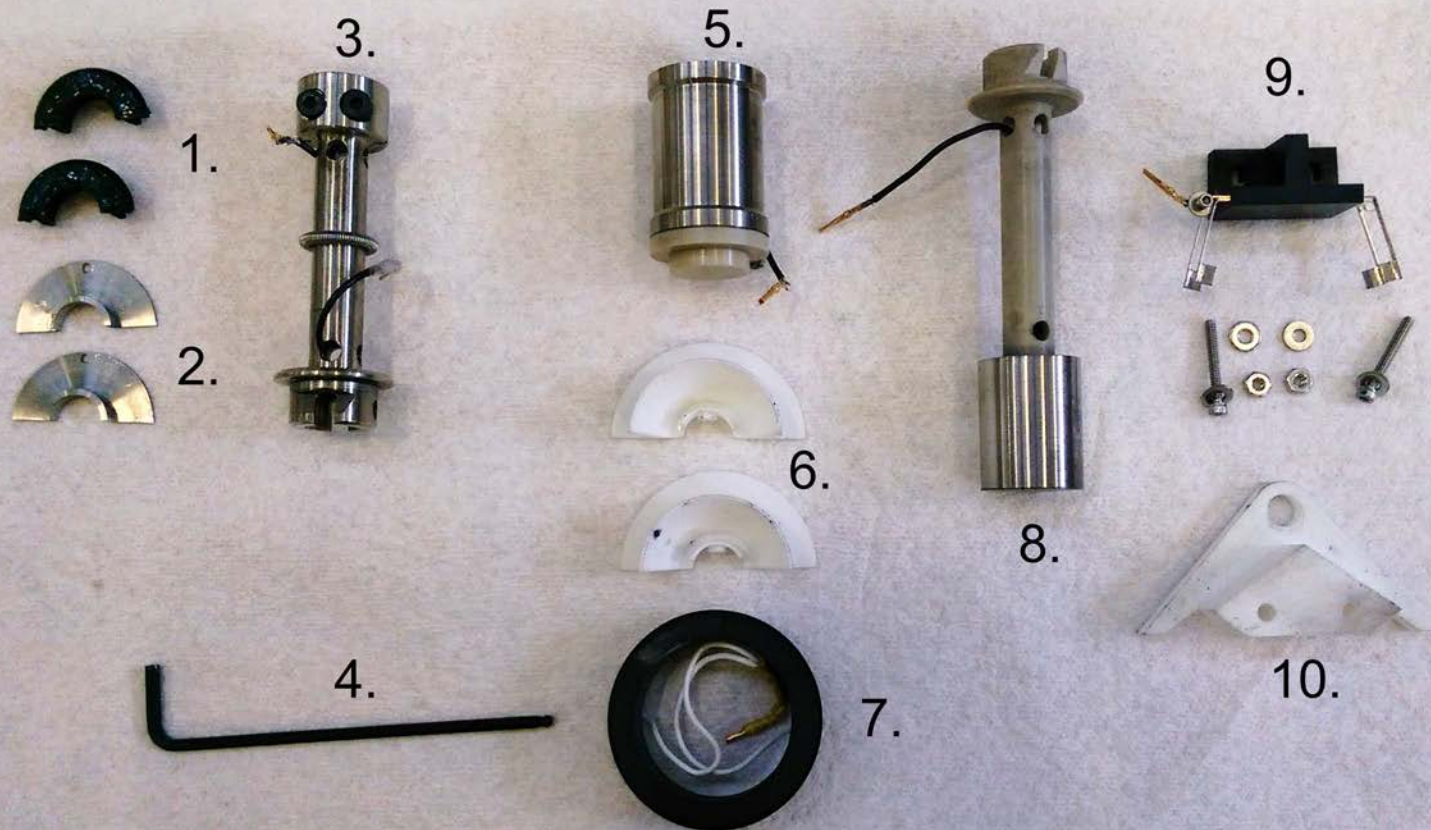


d.)



e.)

- | | | |
|--------------------|----------------|-------------------|
| 1. Transducer Lock | 5. Window | 9. Neutron Guides |
| 2. Motor Lock | 6. Crane Mount | 10. Rheometer |
| 3. Snout Mount | 7. Crane Hook | 11. Detector Tube |
| 4. Huber Table | 8. Cables | |



1. Solvent Trap

2. Wire Baffle

3. Dielectric
Geometry

4. 3 mm Allen Key

5. Dielectric Cup

Assembly

6. Slip Ring Adapter

7. Slip Ring

8. Dielectric Bob

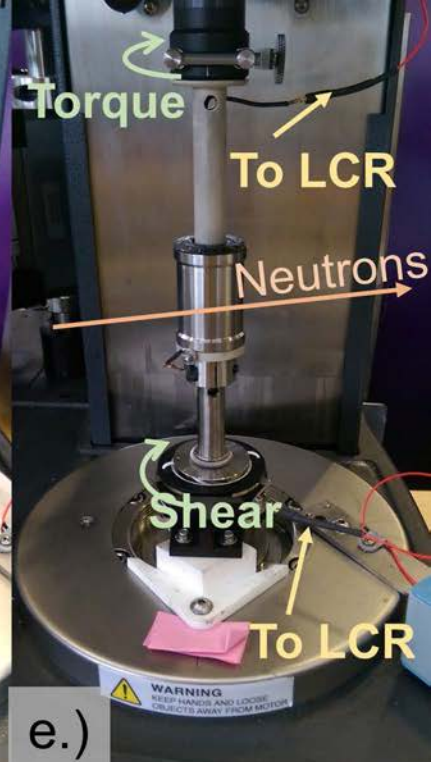
Assembly

9. Carbon Brush

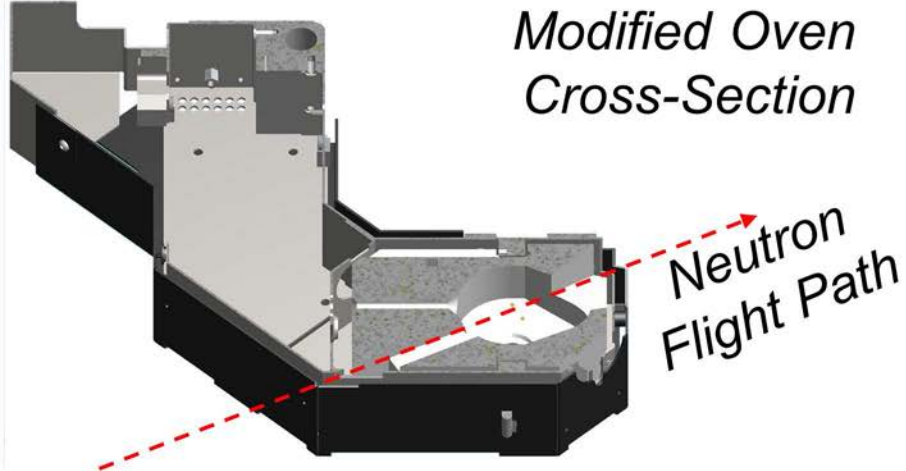
Assembly

10. Carbon Brush

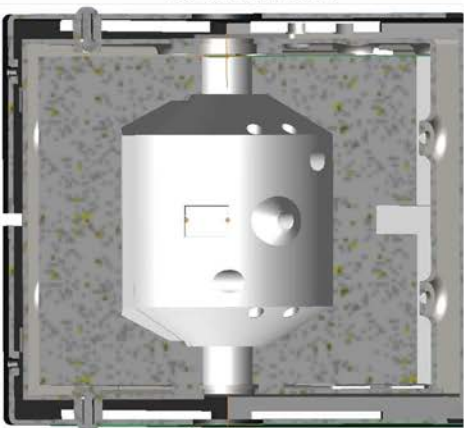
Adapter



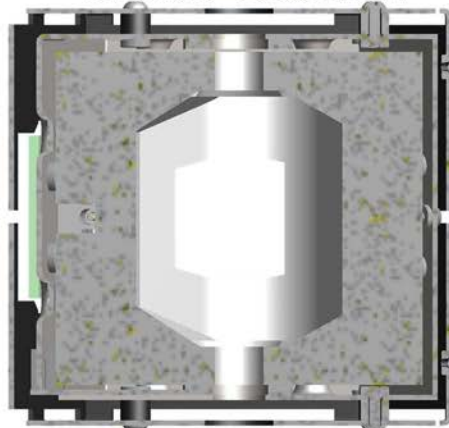
*Modified Oven
Cross-Section*



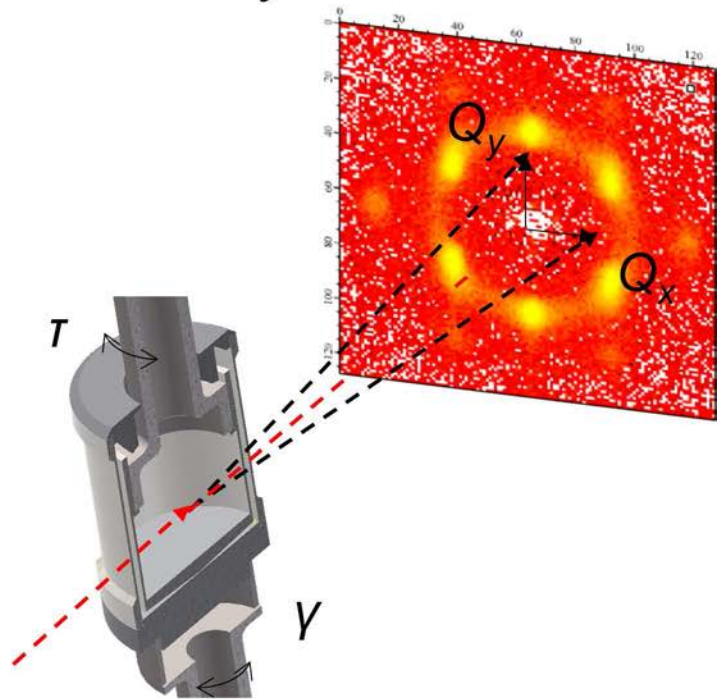
Beam Entry Cross-Section

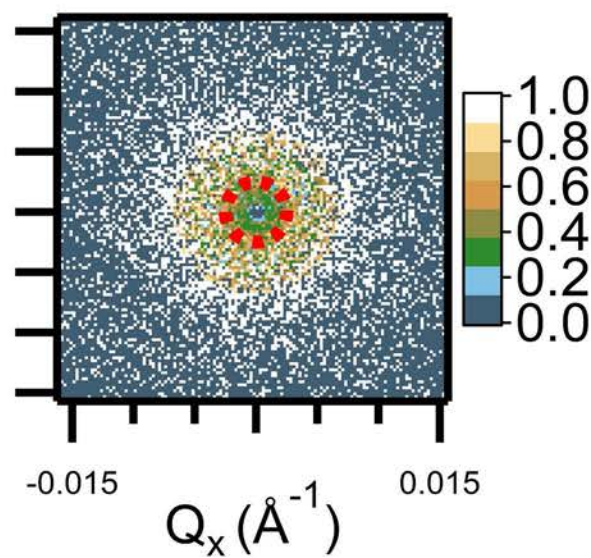
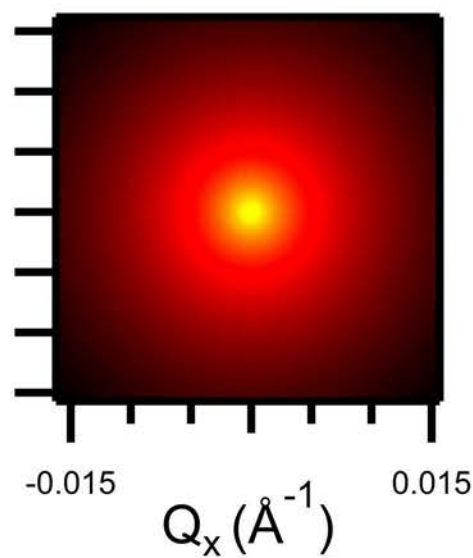
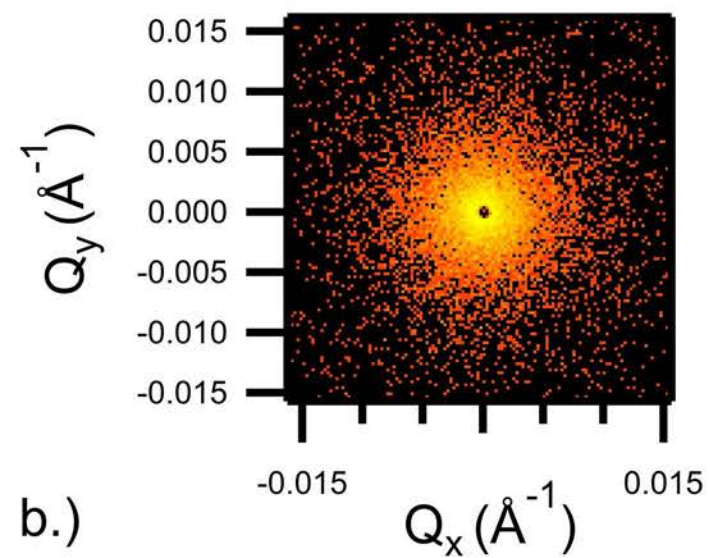
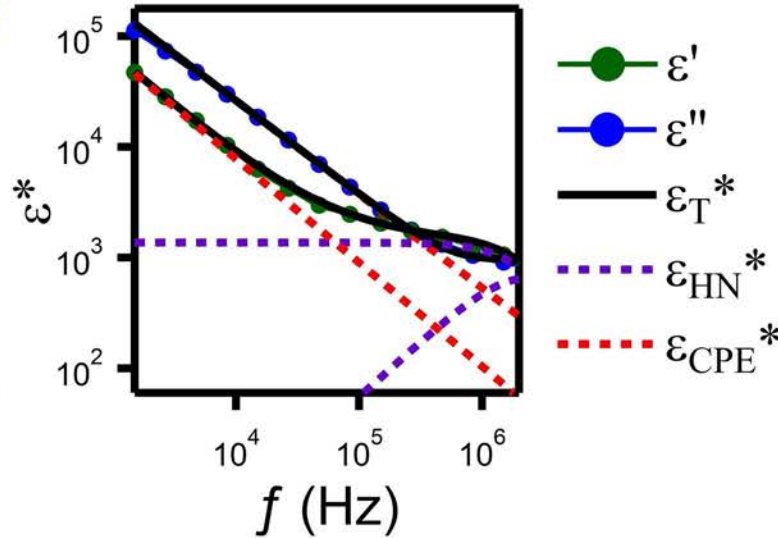
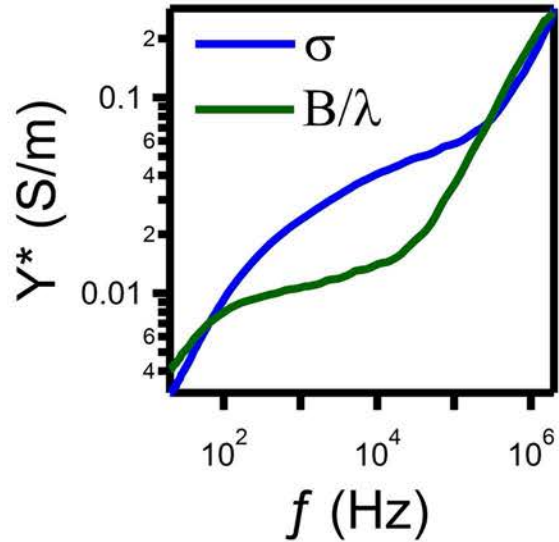
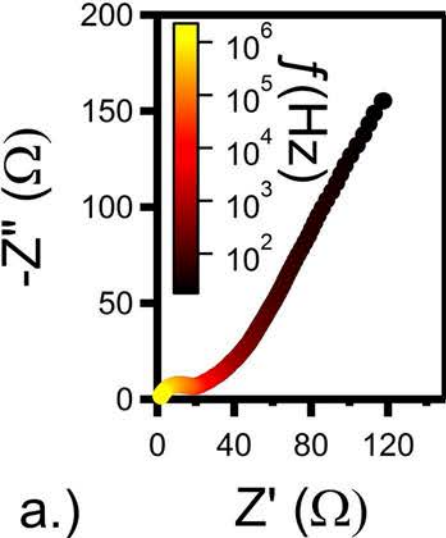


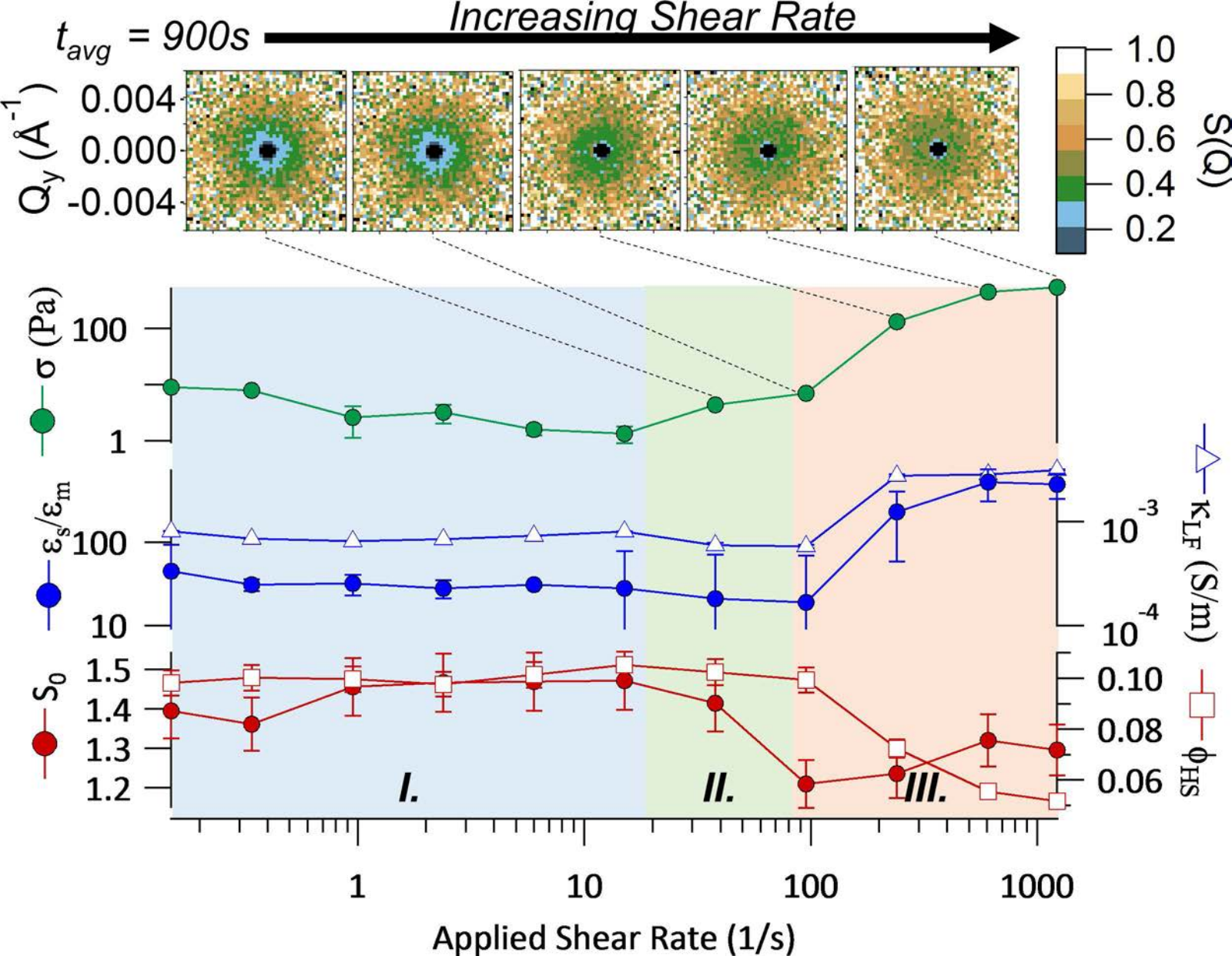
Beam Exit Cross-Section



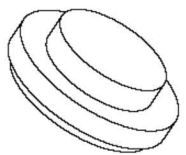
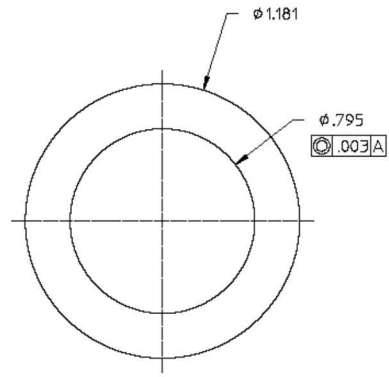
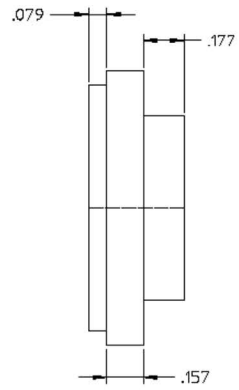
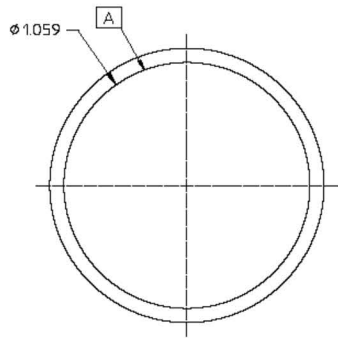
Geometry Cross-Section





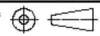


REVISIONS				
No.	ZONE	ECN	CHANGE	DATE
1				

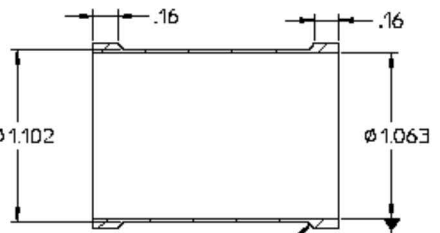


MATERIAL SPECIFICATION		APPROVALS		UNLESS OTHERWISE SPECIFIED DIMENSIONS ARE IN INCHES TOLERANCES ARE: DECIMALS FRACTIONS XXX" = .000 ANGLES AS X" = .1" ANGLES AS		NIST National Institute of Standards and Technology U.S. DEPARTMENT OF COMMERCE		CENTER FOR NEUTRON RESEARCH 10 BUREAU DRIVE ANTWERP, NJ 08846	
NATIONAL PEEK	OVER	DATE	DATE	DATE	DATE	PEEK ADAPTER - ARES			
FORM SHAPE, ROUND	FORM	FORM	DATE	DATE	DATE				
MODEL DATA		DRAWING DATA		DO NOT SCALE DRAWING		FOR			
MODEL NAME	STATUS	DATE	DATE	DRAWER		PART NO.			
CREATING OFFICE	WORK	12/8/15 3:08 PM	12/8/15 3:08 PM	Cedric Gagnon		014-2009			
CREATOR	VERSION	DATE	SHEETS	PHONE NUMBER		SCALE		SHEET	
Cedric	1	12/8/15 5:03 PM	1	(301)975-2020		3:1		1 of 1	
THIRD ANGLE PREDIGIT	DATE	DATE	DATE	EVAL. APPROV.		RELEASE DATE		DIM. & TOL. PER ANSI Y14.5M-1982	
	12/8/15 3:26 PM	12/8/15 3:26 PM	12/8/15 3:26 PM	cedric.gagnon@nist.gov					

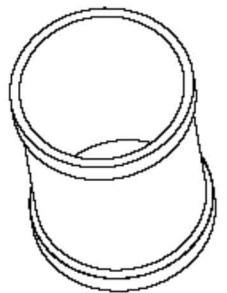
NOTES:



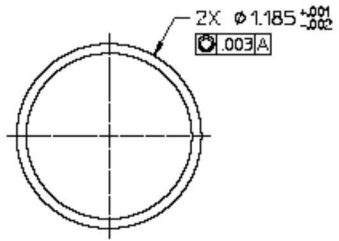
REVISIONS				
NO.	DATE	BY	CHANGE	DATE
2	08-2		ADDED SHOULDER AND CHAMFERS	12/18/75



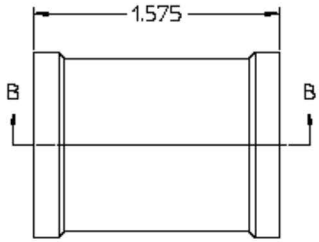
2X 45°x.04
SECTION B-B



GEN1



FRONT1



RIGHT1

NOTES:
1-REMOVE ALL BURRS AND SHARP EDGES.

MATERIAL SPECIFICATION		APPROVALS		UNLESS OTHERWISE SPECIFIED DIMENSIONS ARE IN INCHES TOLERANCES UNLESS OTHERWISE SPECIFIED		NIST National Institute of Standards and Technology U.S. Department of Commerce		CENTER FOR BUSINESS PUBLICATIONS 16150 BELLAIR BLVD. BETHESDA, MD 20814	
ITEM NO. 170000	REV. 1	DATE 02/16/75	BY DGA	DATE 02/16/75	BY DGA	DATE 02/16/75	BY DGA	CAN. CUP - ARES	
PART NAME CAN. CUP		QUANTITY DATA		DESIGNED BY Dedric Goggin		CHECKED BY Dedric Goggin		DATE 13011875-2020	
SIZE 1.185	TYPE CUP	DATE 02/16/75	BY DGA	DATE 02/16/75	BY DGA	DATE 02/16/75	BY DGA	SCALE 2:1	
DRAWN BY DGA		CHECKED BY DGA		DATE 02/16/75		DATE 02/16/75		SHEET NO. 1 of 1	
TOLERANCE PRACTICE AS SHOWN		DATE 02/16/75		DATE 02/16/75		DATE 02/16/75		DPI & TOL. PER ANSI Y14.5-1982	

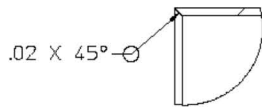
NIST National Institute of Standards and Technology U.S. Department of Commerce		CENTER FOR BUSINESS PUBLICATIONS 16150 BELLAIR BLVD. BETHESDA, MD 20814	
CAN. CUP - ARES			
D14-1828			
REV. B	DATE 08-2	BY DGA	DATE 12/18/75
SCALE 2:1		SHEET NO. 1 of 1	
DPI & TOL. PER ANSI Y14.5-1982			

2

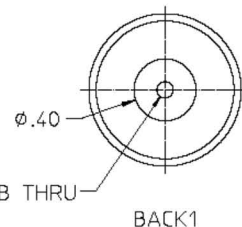
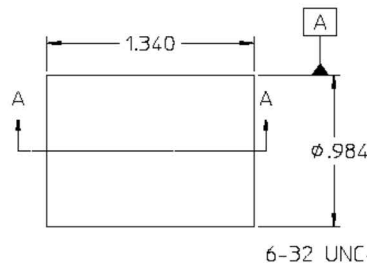
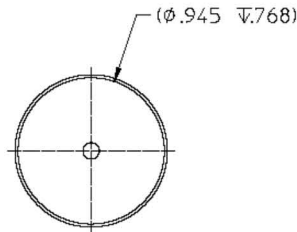
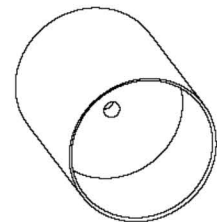
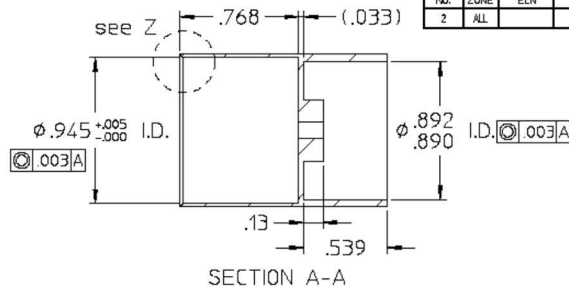
1

1

REVISIONS				
No.	ZONE	ECN	CHANGE	DATE
2	ALL		REVISED CENTER OF PART	2/20/16



Z
SCALE 5:1



NOTES:

1-REMOVE ALL BURRS AND SHARP EDGES.

MATERIAL SPECIFICATION		APPROVALS		UNLESS OTHERWISE SPECIFIED DIMENSIONS ARE IN INCHES TOLERANCES ARE:		NIST		CENTER FOR NEUTRON RESEARCH	
MATERIAL: TITANIUM GRADE 2, REDUCED	FORM: BAR, ROUND	DATE: 2/20/16	DATE: 2/20/16	DECIMALS: .001	FRACTIONS: 1/16	Federal Institute of Standards and Technology U.S. DEPARTMENT OF COMMERCE		TO BUREAU OF METROLOGY NORTHREAR, MD 20899	
MODEL DATA		DRAWING DATA		DO NOT SCALE DRAWING		CAN, BOB - ARES		FOR: D14-1928	
MODEL NAME: TI Bob, 4in	DATE: 8/3/15 12:21 PM	WORK: 2	SHEETS: 2	DRAWER: Cedric Gagnon	PHONE NUMBER: (301)975-2020	B		DATE: 014-1932	SHEET: 1 of 1
CREATOR: cedric	DATE: 8/3/15 12:21 PM	WORK: 2	SHEETS: 2	DRAWER: Cedric Gagnon	PHONE NUMBER: (301)975-2020	SCALE: 2:1	RELEASE DATE:	DIM. & TOL. PER ANSI Y14.5M-1982	
THIRD ANGLE PROJECTION		DATE: 2/20/16 12:31 PM	DATE: 2/20/16 12:31 PM	EMAIL: cedric.gagnon@nist.gov					

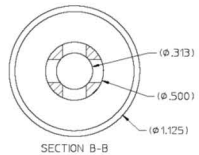
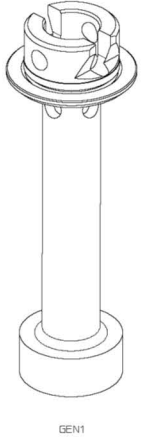
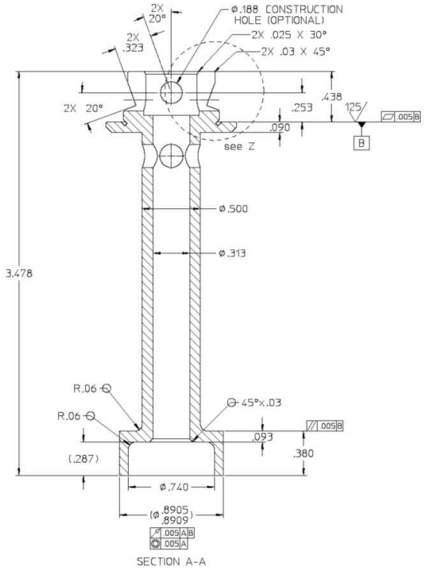
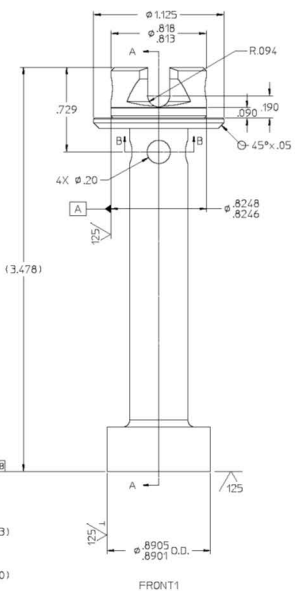
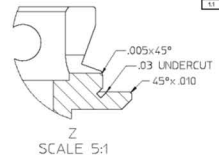
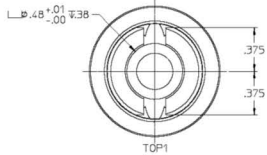
2

1

1

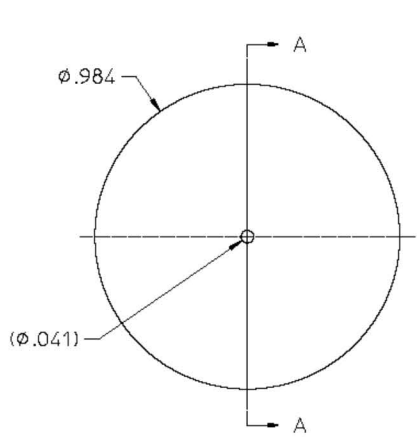
1

REVISIONS				DATE
NO.	ZONE	REV.	CHANGE	
1.1				

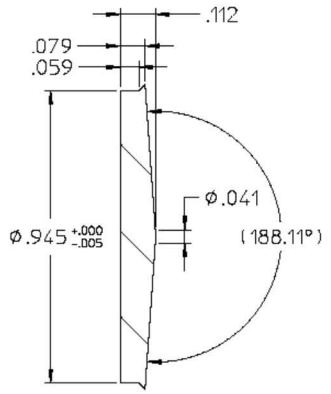


MATERIAL SPECIFICATION		DIMENSIONAL TOLERANCES		SURFACE FINISH		REVISIONS		DATE	
ITEM	QTY	UNIT	DESCRIPTION	FINISH	RA	NO.	ZONE	REV.	DATE
1	1	PC	SHAFT, BOB - ARES	005B	0.8	014-1931			
NOTES:		Z REMOVE ALL BURRS AND SHARP EDGES.		D		014-1931		1.1	

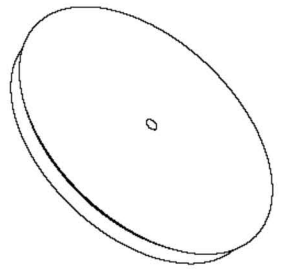
REVISIONS				
No.	ZONE	ECN	CHANGE	DATE
1				



FRONT1



SECTION A-A

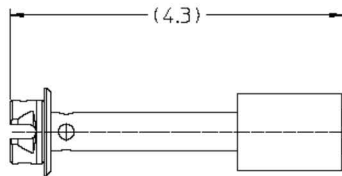


GEN1

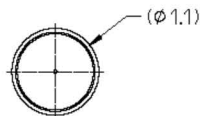
NOTES:
1-REMOVE ALL BURRS AND SHARP EDGES.

MATERIAL SPECIFICATION		APPROVALS		UNLESS OTHERWISE SPECIFIED DIMENSIONS ARE IN INCHES TOLERANCES ARE: DECIMALS FRACTIONS XXX ± .000 ANGLES AS SHOWN	
NATIONAL PEEK	FORM FROM	DATE	DATE	DATE	DATE
FORM ROUND	FORM FROM	DATE	DATE	DATE	DATE
MODEL DATA		DRAWING DATA		DO NOT SCALE DRAWING	
MODEL NAME PEEK bob.cad	DATE 8/3/16 12:21 PM	DATE 8/16/16 11:47 AM	DATE 8/16/16 11:47 AM	DATE 8/16/16 2:30 PM	DATE
CREATOR cadtc	WORKSHEET 1	WORKSHEET	WORKSHEET	WORKSHEET	WORKSHEET
THIRD ANGLE PERSPECTION			DRIVER Cedric Gagnon PHONE NUMBER (301)975-2020 EMAIL ADDRESS cedric.gagnon@nist.gov		

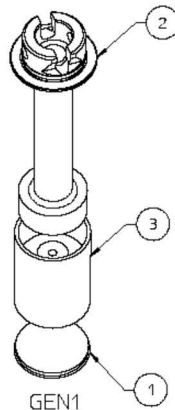
NIST National Institute of Standards and Technology U.S. DEPARTMENT OF COMMERCE		CENTER FOR NEUTRON RESEARCH 10 BUREAU DRIVE Gaithersburg, MD 20899	
CAP, BOB - ARES			
PDR 014-1928			
SEC B	OWN No. 014-1930	REV 1	SHEET 1 of 1
SCALE 4:1	RELEASE DATE	NET. WT.	DIM. & TOL. PER ANSI Y14.5M-1982



FRONT1



RIGHT1



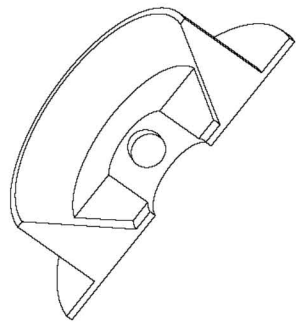
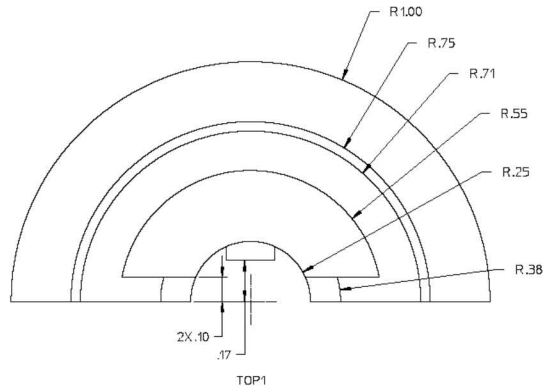
GEN1

REVISIONS				
No.	ZONE	ECN	CHANGE	DATE
2				

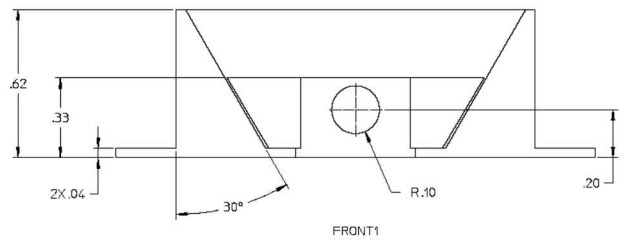
QTY	PART No.	SUPPLIER PART No.	SUPPLIER	DESCRIPTION	MATERIAL	ITEM
1	014-1932	N/A	OPEN MARKET	CAN. BOB - ARES	TITANIUM, GRADE 2, R50400	3
1	014-1931	N/A	OPEN MARKET	SHAFT, BOB - ARES	PEEK	2
1	014-1930	N/A	OPEN MARKET	OPEN MARKET	PEEK	1

MATERIAL SPECIFICATION		APPROVALS		UNLESS OTHERWISE SPECIFIED DIMENSIONS ARE IN INCHES UNLESS INDICATED OTHERWISE		NIST		CENTER FOR NEUTRON RESEARCH		
NATIONAL PER ASSEMBLY	OVER	DATE	DATE	DECIMALS	FRACTIONS	Federal Institute of Standards and Technology		TO BUREAU OF METROLOGY, NIST		
PER ASSEMBLY	FORM	YEAR	DATE	XXX = BOB	XXX = ANGLES	U.S. DEPARTMENT OF COMMERCE		ARES DIELECTRIC BOB ASSEMBLY		
MODEL DATA		DRAWING DATA		DO NOT SCALE DRAWING		FOR		014-1927		
MODEL NAME	STATUS	DATE	VERSION	SHEETS	DRAWER	BOM No.		014-1928		
dielcbrt_bob Assy	WORK	7/16/16 4:47 PM	2	2	Cedric Gagnon	SCALE		1:1		
CREATOR	DATE	TIME	DATE	TIME	PHONE NUMBER	RELEASE DATE		SHEET		
cedric	8/3/16	12:21 PM	7/16/16	4:47 PM	(301)975-2020	NET. WT.		1 of 1		
THIRD ANGLE PERSPECTION	DRAWING DATA		DATE		EVAL. APPROV.		DIM. & TOL. PER ANSI Y14.5M-1982			
	DRAWING DATA		DATE		cedric.gagnon@nist.gov					

REVISIONS				DATE
No.	ZONE	ECN	CHANGE	DATE
1				



GEN1
SCALE 3:1



NOTES:
1. REMOVE ALL BURRS AND SHARP EDGES.

MATERIAL SPECIFICATION		APPROVALS		NET National Institute of Standards and Technology U.S. Department of Commerce		CENTER FOR METROLOGY RESEARCH 400 DuPont Circle Washington, DC 20036	
ITEM:	QTY:	DATE:	DATE:	DESIGNED BY:	DATE:	DRWING NO.:	REV. NO.:
ACQUISITION DATA		MANUFACTURE DATA		SLP RING ADAPTER - ARES 014-1929 C 014-2137 1 of 1 DIM & TOL. PER ANS1 Y14.5M-1982			
PART NAME: SLP RING ADAPTER PART NO.: 014-1929 QTY: 1 DATE: 10/26/2004		DRAWING NO.: 014-1929 REV. NO.: 1 DATE: 10/26/2004 DESIGNED BY: C. GAGNON DRAWN BY: C. GAGNON CHECKED BY: C. GAGNON DATE: 10/26/2004		PROJECT: 014-1929 DRAWING: 014-2137 SCALE: 3:1 SHEET: 1 of 1			

